Aerodynamic Design Optimization Trim Analysis of Canard Conventional Configurations

Michael W. Keith* and Bruce P. Selberg†
University of Missouri-Rolla, Rolla, Missouri

A design study has been conducted to optimize trim cruise flight of high performance general aviation canard aircraft which achieve minimum drag. In order to investigate the advantages and disadvantages of canard configured aircraft, corresponding conventional tail-aft "baseline" aircraft were designed and used for comparison. Two-dimensional coupled lift and drag coefficient predictions of the canard and wing airfoil shapes were obtained by coupling inviscid results from a vortex panel multielement program to a momentum integral boundary layer analysis. By using the results of the two-dimensional vortex panel analysis, a vortex lattice method was employed to predict the finite wing results. The analysis utilized a turbulent airfoil and a natural laminar airfoil, which are two NASA state-of-the-art airfoil sections. The canard aircraft designs give quantitative results of wing and canard loadings, wing-to-canard moment arm ratios, and aspect ratio effects for trim cruise flight for a wide range of wing-to-canard area ratios. Both canard and baseline aircraft achieved a 25-30% improvement in performance over typical current technology aircraft, but high canard loading necessary for trim resulted in slightly poorer cruise performance of the canard aircraft for equal fuel as compared to the baseline designs. However, when takeoff gross weight was held the same by reducing the fuel payload, the canard designs achieved longer ranges than the baselines. The required positive decalage angle between the canard and the wing guarantees that the canard will stall first, thereby preventing the wing from stalling, and thus having a stall- and, hence, spin-proof configuration.

Nomenclature

a.c.	= aerodynamic center
AR	= aspect ratio
c.g.	= center of gravity
C_d	= sectional drag coefficient
C_{D_i}	= induced drag coefficient
C_D	= total drag coefficient
C_l	= sectional lift coefficient
C_L	= total lift coefficient
C_{L_α}	= total lift curve slope
C_M	= pitching moment coefficient
C_{M_α}	= longitudinal stability derivative
D	= decalage angle
$\bar{G}$	= gap
L/D	= total lift-to-drag ratio
$(L/D)_{max}$	= maximum lift-to-drag ratio
R	= range
R_c	= Reynolds number based on chord
R_e	= Reynolds number per unit length
$\bar{S}$	= stagger
S	= reference area
V	= velocity
W/S	= wing loading
Wt	= weight
X	= moment arm
λ	= taper ratio

Subscripts

C	= canard
CR	= cruise
H	= horizontal tail
W	= wing

Received March 16, 1983; revision received Oct. 20, 1983.

*Former Graduate Student, Mechanical and Aerospace Engineering Department; currently, Engineer, Gates Learjet. Member AIAA.

†Professor of Aerospace Engineering, Mechanical and Aerospace Engineering Department. Associate Fellow AIAA.

Introduction

CANARD aircraft have attracted the interest of designers from time to time because of several particular characteristics. The first powered canard aircraft design began and ended with the Wright Flyer. That aircraft, unfortunately, was longitudinally unstable and the misconception arose that all canard aircraft would be statically unstable in pitch, regardless of the two lifting surfaces. Thus, in the early years of aircraft development, the canard concept was dropped in favor of conventional tail-aft designs. It was not until the 1960's that canards were again seriously considered for high-speed designs. Primarily this was due to the successfully flying canard designs of Rutan.[1,2] Canards have not, however, been widely applied to either transport or light aircraft. Rutan has clearly demonstrated with his homebuilt "sport aircraft" that canard configured aircraft can be longitudinally stable and can have very desirable stall characteristics.

It is desirable to increase efficiency of general aviation aircraft, and this can be done by decreasing trim drag. Laitone[3] points out that minimum trim drag for conventional tail-aft aircraft corresponds to a positive load on the tail. Such aircraft, however, lack a tail volume large enough to permit rearward center of gravity (c.g.) location that would produce an upload on the tail and still permit longitudinal stabilization. It would, therefore, be logical to increase the size of the horizontal tail to provide the required stability margin for the more aft c.g. location, but, as Goldstein and Combs[4] point out, the profile drag and weight penalties associated with the larger tail tend to reduce the benefits. The use of the canard relieves the problem because the trim load is positive and helps reduce the wing lift. As Wolkovitch[5] points out, stability can be attained with any ratio of canard to main wing area, but the resulting c.g. position may demand an excessively high lift coefficient on the canard. These would cause higher induced drag for the canard. At even higher angles of attack the canard boundary layer will separate, causing increases in profile drag. In contrast to the downloading tail-aft configuration, two lifting surfaces

should increase maximum lift, thereby reducing the total wing area (also wetted area). Tulinius and Margason[6] say that the primary emphasis in reducing skin friction drag is placed on minimizing wetted area.

Even with the few successful flying canard aircraft, little quantitative data are available in the literature. It is thus the purpose of this paper to analyze and present detailed analyses of trim cruise flight of high performance general aviation canard aircraft that achieve minimum drag and to compare the results to a tail-aft baseline aircraft designed to the same specifications. The design specifications for both the baseline and the canard six-place aircraft are shown in Table 1. Since two airfoils are to be analyzed, four aircraft will be designed.

Design of the Baseline Aircraft

Fuselage Layout

The fuselage cabin of the six-place aircraft was sized to present minimum frontal area, reducing form drag, while providing adequate interior volume for the pilot, passengers, and baggage. The cabin was designed to accommodate men falling at or below the ninety-fifth percentile in terms of size. The cabin is 132 cm (50 in.) high, 112 cm (44 in.) wide, and 4.42 m (14.5 ft) long, contains six seats in three rows of two seats each, and has the baggage compartment aft of the last two rows of seats. The seat pitch was 91.4 cm (36 in.). The cabin was designed for a pressure altitude of 2438 m (8000 ft); cabin pressure altitude to be maintained to a cruise altitude of 12,192 m (40,000 ft). The rest of the fuselage was sized to provide enough space to enclose the landing gear, powerplant, avionics, and environmental control unit. The fuselage was designed for a retractable tricycle landing gear, the nose gear housed below and forward of the pressure cabin, and the main gear retracting below and aft of the baggage compartment. The main landing gear width is 2.62 m (8.6 ft) and exceeds the FAR overturning criterion. The single turboprop engine is located in the section of the fuselage tail cone furthest aft, and has air inlets and exhausts on either side of the fuselage with the propeller shaft extending through the aft fuselage. The avionics and the environmental control unit were also housed in the fuselage aft of the pressure cabin. One smaller door is located on the left which accesses the first row of seats, and a larger door is located on the right which accesses the two aft rows of seats.

Engine Selection

The six-place aircraft uses a scaled version of the Pratt and Whitney PT6A-45A turboprop engine[7] with a 2.29 m (90 in.) diameter four-bladed propeller. Specific fuel consumption was assumed to be constant 0.344 kg/hw-h (0.55 lb/hp-h). The engine weight was scaled by the ratio of required power to production power. The propeller was used in the pusher mode with the PT6A-45A engine. The engine weights were held constant for both configurations.

Aircraft Weights

The aircraft weights were estimated with the aid of equations given by Nicolai[9] and Torenbeek,[10,11] and from a University of Missouri-Rolla (UMR) design project,[12] a four-place high speed general aviation aircraft, that utilized NASA Structural Analysis prediction methods for lifting surface weights.

The fuselage and empennage weights were determined for the aircraft by using Nicolai's equations with the UMR four-place design as a reference aircraft. Nicolai's equations were used as scaling factors on the reference weights by accounting for the different fuselage dimensions, takeoff weights, and other important factors. The scale factors used were the average for commercial subsonic aircraft and light utility aircraft. Wing weights were estimated from a modification of Torenbeek's formula to account for composite wings, which were used on both aircraft designs. These modified composite wing weight formulas were checked against the results of a NASA internal memo[14] and showed good agreement. Subsequent NASTRAN/SEMOBEAM calculations have validated these results.[14] An ultimate load factor of 5.7 was used and was calculated from a 3.8 g load with a factor of safety of 1.5. Weights of landing gear, avionics, electrical and fuel systems, and other equipment onboard were estimated with Nicolai's equations. The weight of the required fuel was obtained by estimating takeoff and climb fuel consumption, cruise fuel consumption for a range of 1500 mi, descent and approach fuel consumption, and allowing for 20% fuel reserves.

Aerodynamic Methodology

The aerodynamic investigation was completed by using an inviscid vortex panel multielement program, which was coupled to a momentum integral boundary layer analysis program. These predicted theoretical two-dimensional inviscid and viscid data. The results of the two-dimensional vortex panel analysis was used as input to a three-dimensional vortex lattice program to predict the induced drag of the finite lifting surfaces. The multielement vortex panel and vortex lattice programs were used in order to predict the aerodynamic coupling between the canard and the wing surface.

The laminar flow portion of the momentum integral program uses Thwaites' method[15] with Michel's transition criterion.[16] The turbulent flow solution is obtained by Head's momentum integral method[17] with the two-dimensional drag being calculated by the Squire-Young formula.[18] To check the validity of the predicted two-dimensional drag, the analytical results were compared to experimental results[19,20] known at the same Reynolds number for smooth airfoils. Figure 1 compares the theoretical to the experimental data for the

Table 1 Design specifications

Parameter	Range of value
Cruise velocity, V_{CR}	563 km/h (350 mph)
Cruise range, R	2414 km (1500 mm)
Cruise payload, Wt_{CR}	5338 N (1200 lb)
Wing loading, W/S	1197-2873 N/m^2 (25-60 lbf/ft^2)
Aspect ratio, $\mathcal{R}$	6-12
Altitude range	9,144-12,192 m (30-40 kft)
Airfoil sections	NLF-0215F (natural laminar flow airfoil) MS1-0313 (medium speed turbulent airfoil)

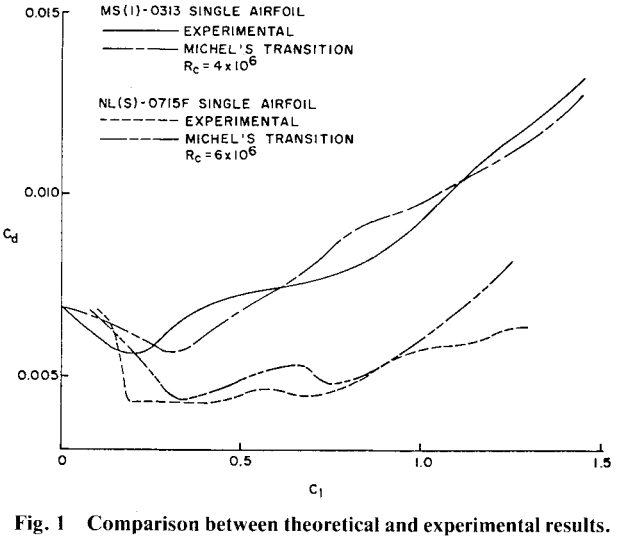

Fig. 1 Comparison between theoretical and experimental results.

MS(1)-0313 airfoil at a Reynolds number, R_c, of 4×10^6 and for the NL(S)-0715F airfoil at a Reynolds number of 6×10^6. (The NL(S)-0715F has recently been renamed the NLF-0215F.) This good agreement was achieved by using a Young's factor of 2.4 for the MS(1)-0313 and a Young's factor of 2.2 for the NL(S)-0715F in the Squire-Young equation. The same good agreement was obtained for both airfoils at other Reynolds numbers.

The vortex lattice program used on this study was developed at UMR. It predicts higher values of induced drag than does a vortex lattice program, NARUVLE, developed by Tulinius,[21] which underestimates induced drag.[22] Figure 2 presents a wing fuselage model $\mathcal{R}=8.9$, and compares the UMR program with NASA data.

The drag for the two aircraft was estimated by using the component buildup method. The drag coefficient of each component was totaled and increased by a factor of 10% to account for interference effects as suggested by Roskam.[23] The drag coefficient for the nonlifting components, which included the fuselage, nacelles, and vertical tail, was estimated from graphs and equations for turbulent flow about streamlined bodies from Roskam,[23] Hoerner,[24] and Crawford.[25] The drag coefficients of the lifting surfaces were predicted by the momentum integral boundary layer program and the vortex lattice program as previously described. For each cruise lift coefficient investigated, the two-dimensional drag at the proper Reynolds number and the induced drag at the desired aspect ratio and taper ratio were added to get a total wing drag coefficient. To account for wing interference, a factor of 10% of the zero-lift drag coefficient for the two airfoils considered was added to the total wing drag coefficient.

The wings of the aircraft were designed to utilize winglets to reduce the induced drag. The magnitude of the induced drag reduction was determined by a computer tradeoff study, which also found the optimum wing taper ratio, λ, at a wing of aspect ratio 12 with taper ratio between 0.2 and 1.0, using the NARUVLE vortex lattice program to compute the induced drag for the various configurations. The parametric analysis yielded an optimized configuration that agreed with Whitcomb[26] in terms of dihedral and incidence, although the magnitude of the predicted drag reduction was less. Because of the high degree of correlation between the current study and the NASA study, the standard NASA winglet design of Whitcomb[26] was used. To be conservative, however, the drag reduction value obtained from NARUVLE was used instead of the value indicated by Whitcomb.[26] These results indicate that $\lambda=0.6$ produces the greatest reduction in induced drag, ΔD_i, below $C_L=0.44$ and $\lambda=0.8$ produces the greatest reduction above $C_L=0.44$. Since it was anticipated that the cruise lift coefficients would be 0.4 or higher, $\lambda=0.8$ was selected over $\lambda=0.6$. The induced drag values of the UMR program were modified to account for the effects of adding winglets using the results of the NARUVLE winglet study, giving a 15% reduction of the wing-induced drag.

Wing Sizing

With the basic fuselage sized, drag coefficient methodology established, and weights estimated, the reduction of configuration drag was completed by optimizing the wing for minimum cruise drag. This included an investigation of taper ratio, winglets, aspect ratio between 6 and 12, and altitude between 9,144-12,192 m (30-40 kft) and staying within the limit of wing loading of 1,197-2,873 N/m^2 (25-60 lbf/ft^2). The aircraft were designed only for achieving a high-speed, fuel-efficient, long-range cruise mission by matching the airplane design to cruise performance requirements. It has been shown[27,28] that engines which meet the cruise design requirements would be flat rated to meet typical general aviation field length requirements. The cruise weight consisted of the aircraft with a full payload plus 20% reserve fuel and half the available fuel above reserve.

The optimization of wing area and altitude for minimum cruise drag was accomplished by the use of a computer program which computed a wing weight for each wing area in the desired range and then found the total aircraft weight. This allowed a corresponding lift coefficient to be calculated. At this lift coefficient, the program searched through two- and three-dimensional drag polars to find the two- and three-dimensional drag coefficient for the specific conditions of Reynolds number (altitude) and aspect ratio. The drag of the nonlifting components was computed and added to the wing drag. Searching for the minimum drag then gives the configuration which has maximum range for a fixed amount of fuel.

Figure 3 shows a sample of the results of the optimization program for the six-place aircraft configured with the MS(1)-0313 airfoil section and aspect ratio of 8 and 12. Over a wing area range of 6.9 to 27.6 m^2 (75 to 300 ft^2), the minimum cruise drag was obtained at an area of 13.9 m^2 (151.6 ft^2) for the wing with $\mathcal{R}=8$ and 12.7 m^2 (138.6 ft^2) for the wing with $\mathcal{R}=12$. The figure also indicates the significant drag

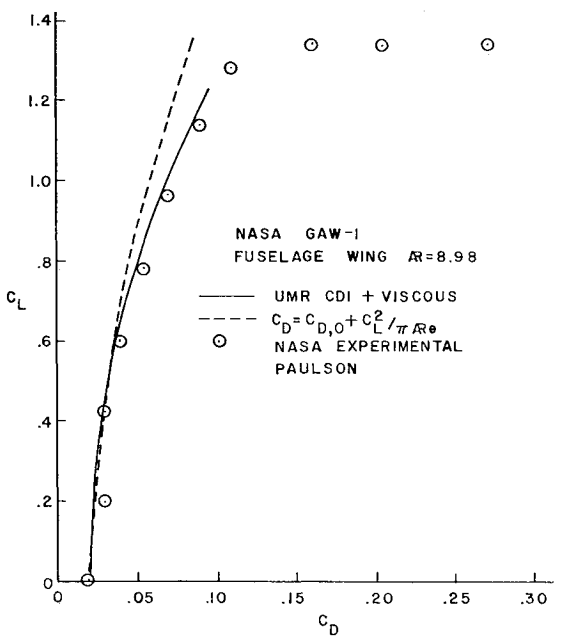

Fig. 2 Vortex lattice program comparison.

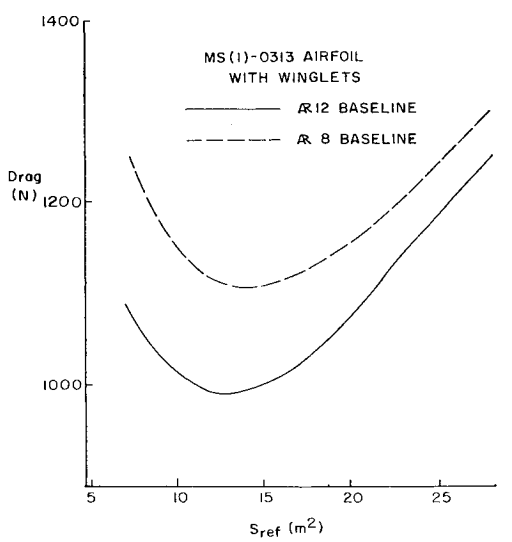

Fig. 3 Sample optimization curves for the six-place baseline aircraft.

reduction, about 10%, achieved by increasing the aspect ratio from 8 to 12.

Based on the results obtained by the optimization program, an altitude of 12,195 m (40,000 ft) was selected as being the best cruise altitude. Since the aircraft were arbitrarily limited to an aspect ratio of 12 or less, an aspect ratio of 12 was chosen for its low minimum drag values.

Stability and Control/Tail Sizing

Using the techniques of Roskam,[29,30] a static stability program was generated which aided in determining the wing location, horizontal and vertical tail sizes, and static stability derivatives. Accounting for the aerodynamic center (a.c.) shift due to the body and all possible loading conditions at cruise flight, longitudinal, lateral, and directional stability were obtained which are comparable to that found on typical light and business aircraft. No dynamic analysis was performed.

Trim

The trim performance was completed by obtaining a zero pitching moment at cruise flight conditions. This was accomplished by finding the required tail lift coefficient for trim flight and the two- and three-dimensional drag associated with it. The additional trim drag was calculated, and the untrimmed data obtained from the optimization program were modified accordingly.

Design of the Canard Aircraft

Ground Rules

The canard aircraft were designed to meet the same objectives as outlined for the baseline aircraft. Each used the same fuselage, vertical tail, and engines as the baseline aircraft. The canard aircraft were optimized for 12,195 m (40,000 ft). The canard and wing have a taper ratio equal to 0.8, while only the wing utilized winglets. Since the canard is forward of the c.g., winglets were not used on the canard, thus maintaining the same directional stability as the baseline without increasing the vertical tail size. The aspect ratio was defined individually for both lifting surfaces as the square of the individual span divided by the reference area of the individual lifting surface. The component weights of the canard aircraft are identical to the baseline aircraft except for the lifting surface weights. Each lifting surface weight was estimated as described for the baseline aircraft, but based on the maximum percentage load it carried. There were two versions of the six- and twelve-place canard aircraft. One version utilized the MS(1)-0313 airfoil for both the canard and wing, while the other version utilized the NL(S)-0715F airfoil on both lifting surfaces.

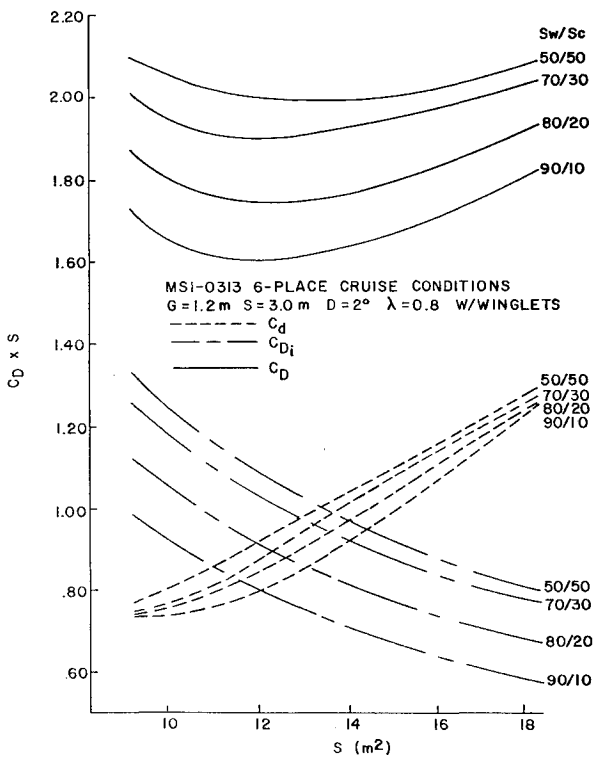

Fig. 4 Weighted drag coefficient for the six-place NS(1)-0313 canard aircraft.

Canard Selection

The terms associated with the design and location of the canard and wing are gap $\bar{G}$, stagger $\bar{S}$, and decalage D. Gap is the vertical distance between the canard and wing and is always considered positive. Stagger is the horizontal distance between the canard and the wing with positive stagger oc-

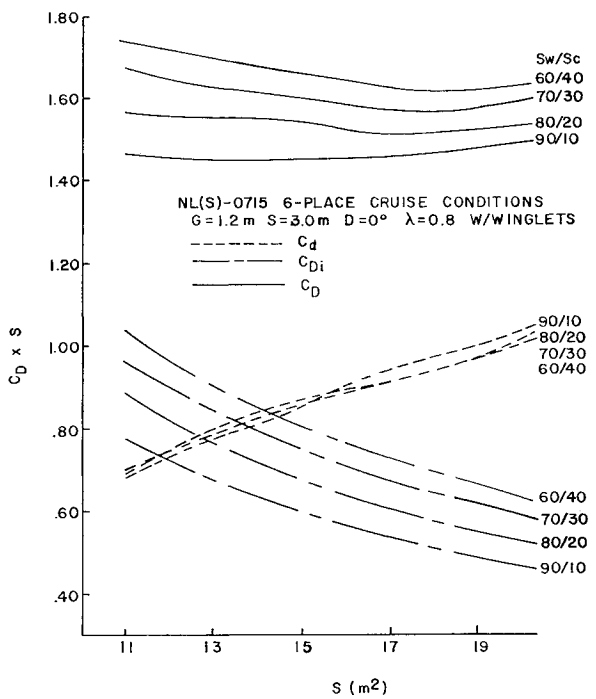

Fig. 5 Weighted drag coefficient for the six-place NL(S)-0715F canard aircraft.

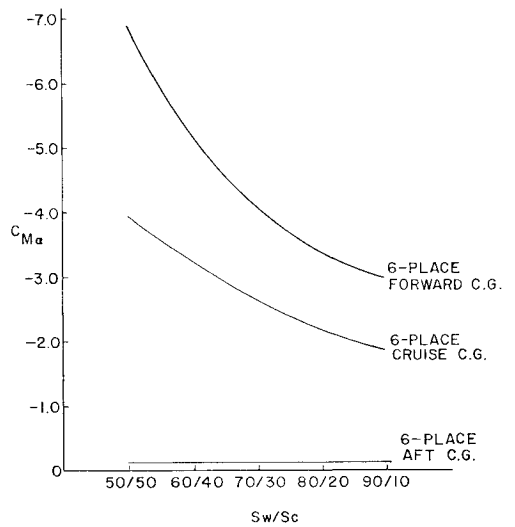

Fig. 6 Longitudinal stability derivative for the canard aircraft.

curring when the canard is above the wing. Decalage is the relative angle of attack between the canard and wing, positive when the canard is at a higher angle of attack than the wing. Both gap and stagger are measured from midchord to midchord. The dividing line between canard and tandem wing configurations is somewhat arbitrary and not really important here. For this design study, it is assumed that a canard configuration is one in which the forward surface acts as the horizontal stabilizer and the configuration does not have an aft horizontal control surface. Also, any configuration with a stagger less than two wing chord lengths is considered to be a dual wing configuration.

An aerodynamic tradeoff analysis of canard aircraft designs by Keith[31] was conducted to obtain "flyable" aircraft with minimum cruise drag. Consideration was given to certain design constraints such as: canard and wing as related to gap and stagger; stability and control which determined the possible locations of the wing and canard; and trim, stall, and takeoff rotation, which determined the decalage angle and wing-to-canard area ratio. The tradeoff results of Keith[31] suggested a canard configuration with the highest possible wing-to-canard area ratio, a decalage slightly less than 0 deg, and the largest gap and stagger possible.

Wing Sizing

Since the altitude and wing taper ratio were optimized in the baseline study, only the total wing area was optimized and selected to obtain minimum cruise drag for the canard aircraft. Figures 4 and 5 show the weighted drag coefficient ($C_D \times S$) as a function of the total wing area considered for various wing-to-canard area ratios. These figures present the breakdown of the two-dimensional and induced drag coefficient as well as the total drag coefficient for the canard aircraft with the MS(1)-0313 airfoil and NL(S)-0715F airfoil, respectively. Figure 4 shows that the MS1 two-dimensional drag increases at almost the same rate as the three-dimensional induced drag decreases, with increasing wing area. The minimum total drag occurs close to the intersection of the two drag components, at which point the two are equal, i.e., a total wing area between 11.9 m^2 (130 ft^2) and 13.8 m^2 (150 ft^2) for all wing-to-canard area ratios. However, the NL(S)-0715F two-dimensional drag does not increase as rapidly as does the MS(1)-0313 two-dimensional drag for increasing wing area because of the large and shallow two-dimensional drag bucket of the NLS airfoil section. This also results in a large shallow drag range for the NLS version of the canard aircraft as illustrated in Fig. 5. Since the induced drag decreases more rapidly than the two-dimensional drag increases, however, the minimum drag for the NLS version occurs at a wing area equal to 18.4 m^2 (200 ft^2), a much higher total wing area than for the MS1 version.

Stability and Control

Shown in Fig. 6 is the longitudinal stability derivative, C_{M_α}, for the six-place canard configuration. This figure shows the changing degree of longitudinal stability for the forward, aft, and cruise c.g. positions for the various wing-to-canard area ratios; it ranges from $-7.0 < C_{M_\alpha} < -0.1$. Longitudinal stability for most subsonic aircraft range from $-3.0 < C_{M_\alpha} < -0.1$. The longitudinal stability of the configurations with lower wing-to-canard area ratios is affected more by the c.g. travel than the configurations with higher wing-to-canard area ratios. Even though the more tandem configurations are statically stable for all possible flight conditions, pilots may not like the large difference in response due to the c.g. travel.

To achieve longitudinal stability at different values of stagger, each wing-to-canard area ratio must have a different ratio of canard moment arm to wing moment arm, X_C/X_W. Figure 7 shows the a.c. locations for the wing and canard at minimum, maximum, and design stagger. The distance between the wing and canard is the stagger and can be directly obtained from Fig. 7. Stagger decreases as S_W/S_C increases. Notice that as the canard is moved forward, the wing must correspondingly be moved aft, causing an increase in stagger. Keith[31] had shown that it would be desirable to go with the largest possible stagger, but placing the canard near the nose of the aircraft was not possible or practical due to the nose gear and windshield locations and the restriction of the pilot's view. Thus stagger was limited to smaller than optimum distance. Since a high canard is aerodynamically desirable, the location of the canard was selected just aft of the windshield. The stability analysis was completed, as it was for the baseline aircraft, using the methods of Roskam[29,30] and modifying the stability program to account for the canard, rather than the aft horizontal tail. Because of the large moment arm needed

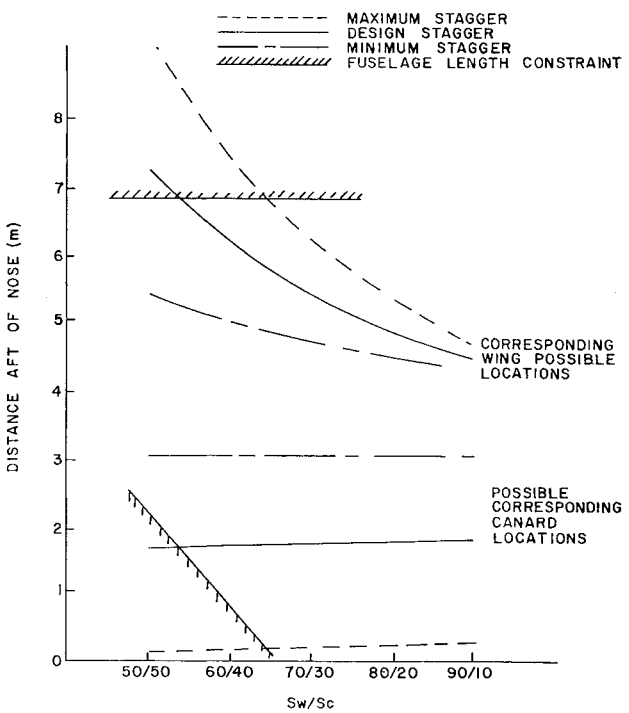

Fig. 7 Wing and canard corresponding a.c. locations that achieve similar longitudinal stability for the six-place canard aircraft.

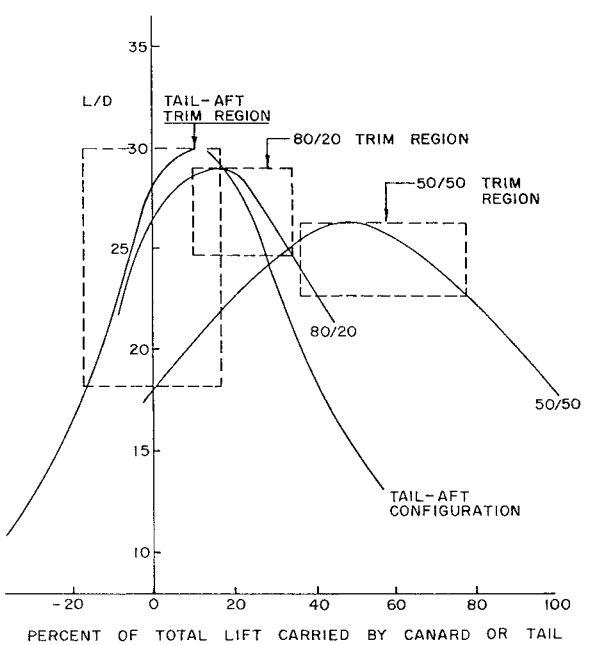

Fig. 8 Trim comparison between canard and tail-aft configurations.

on the wing at wing-to-canard ratios less than 80/20, the fuel could not be placed in the wing without creating a very large c.g. travel or an unstable aircraft. For these wing-to-canard area ratios, a fuel cell was located aft of the cabin. The fuel could, however, be placed in both lifting surfaces; this, however, would require a fuel regulator from both the canard and wing such that the c.g. range remain acceptable with the fuel flow rate.

The final and deciding design criterion for the canard configuration was the analysis of trim. Trim did not produce any additional drag, just dictated the decalage angle needed for cruise level flight. Figure 8 shows the trim regions for canard configurations with wing-to-canard area ratios of 50/50 and 80/20, and also the trim region for a comparable conventional tail-aft configuration. These results were obtained from the unoptimized baseline and canard designs for the six-place aircraft with the MS(1)-0313 airfoil having equal reference areas of 100 ft^2. The canard designs include a region of trim decalage from -4 to 4 deg, while the tail-aft configuration includes a trim region of horizontal tail lift coefficient $-0.3 < C_{L_H} < 0.3$. This figure shows how the off-optimum load penalizes the conventional tail-aft as compared to the canard configurations. For minimum L/D for trim of the canard design is much higher than the tail-aft design also at minimum L/D for trim.

Figure 9 shows the zero moment coefficient as a function of decalage angle (i.e., elevator deflection) for different wing-to-canard area ratios. The pitching moment is very sensitive with decalage angle or elevator deflection of wing-to-canard area ratios of 70/30 or less. However, equally important is the fact that for trim the canard must be at a higher angle of attack than the wing. Thus, the canard will stall first, causing the aircraft to pitch down, but without losing the main lift from the wing. Thus, for canard configurations using the same airfoil shape on both lifting surfaces, the aircraft is not stallable and hence is spin-proof. This is significant, since approximately 30% of the general aviation fatalities are due to stall-spin occurrences.

Rutan[1] points out that in order to satisfy trim static longitudinal stability requirements, the value of wing loading divided by the slope of the lift curve must be higher on the canard than the wing, $(W/S)_C/C_{L_{\alpha C}} > (W/S)_W/C_{L_{\alpha W}}$. This, he asserts, is the primary reason why his stall-proof canard aircraft have been successful, and why those of other canard designers have not. This was also true for the canard designs of this study. The canard ratio, $(W/S)_C/C_{L_{\alpha C}}$, was 1½ times greater than the wing ratio, $(W/S)_W/C_{L_{\alpha W}}$, at a wing-to-canard area ratio of 50/50 and was four times greater at an area ratio of 90/10. Because the same airfoil is used on the canard and wing, the canard-to-wing lift curve slope ratio, $C_{L_{\alpha C}}/C_{L_{\alpha W}}$, remains almost equal for different total areas and area ratios, and was only slightly greater than one. This implies that the canard loading must be greater than the wing loading, $(W/S)_C > (W/S)_W$. The ratio of canard loading to wing loading was approximately equal to 2 at an area ratio of 50/50 and approached a value of 5 at an area ratio of 90/10. The canard loading to wing loading ratio did decrease with decrease in total area for all area ratios.

Since static longitudinal stability depends primarily on the lift curve slopes and the location of the two lifting surfaces, a range of aspect ratio was analyzed for the wing and canard with the anticipation of alleviating the high induced drag of the canard that was encountered at the large area ratios. As the wing aspect ratio, $\mathcal{R}_W$, decreases or the canard aspect ratio, $\mathcal{R}_C$, increases, $C_{L_{\alpha C}}/C_{L_{\alpha W}}$ increases. However, to maintain similar longitudinal stability, stagger must increase as $\mathcal{R}_W$ or X_C/X_W decreases and $(W/S)_C/(W/S)_W$ increases. This is illustrated in Fig. 10. A first impression is that

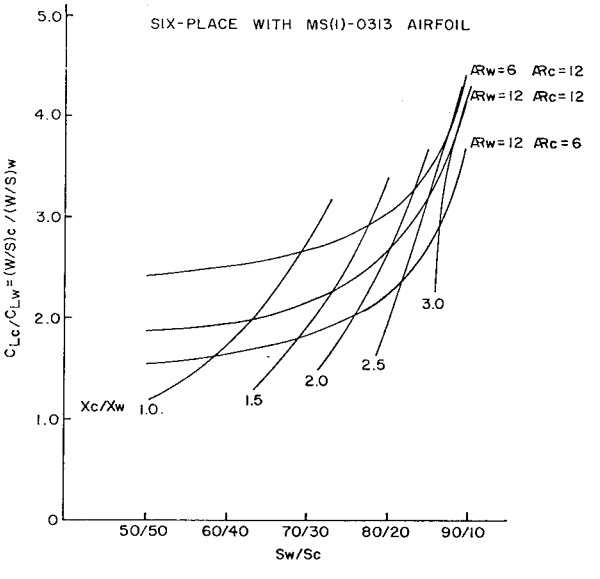

Fig. 10 Canard-to-wing loading ratio with different combinations of wing and canard aspect ratio.

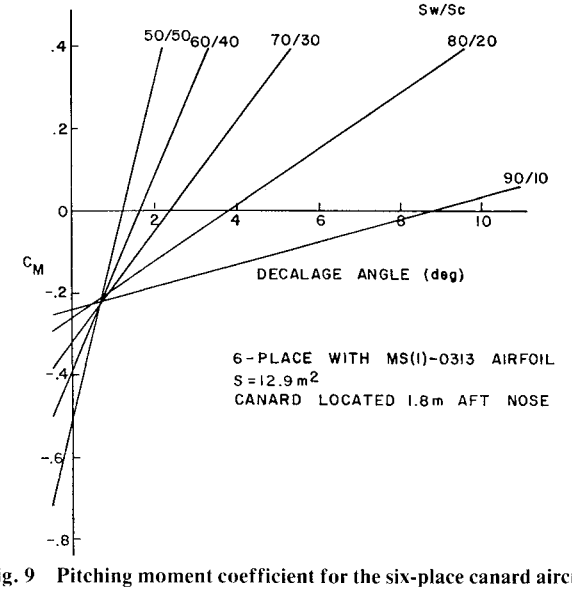

Fig. 9 Pitching moment coefficient for the six-place canard aircraft.

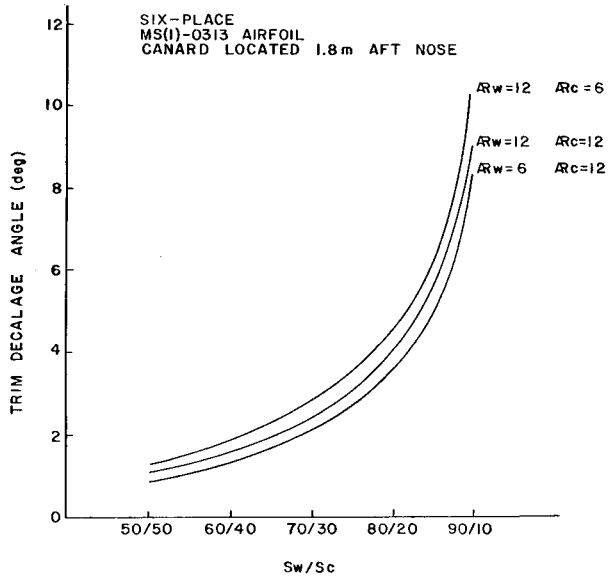

Fig. 11 Trim decalage angle with different combinations of wing and canard aspect ratio.

an increase in $(W/S)_C/(W/S)_W$ would also increase the drag, but because of the high values of $C_{L_{\alpha C}}/C_{L_{\alpha W}}$ due to increase in AR_W decalage angle for trim, this decreases as illustrated in Fig. 11 for the six-place canard configuration with the MS1 airfoil. For the six-place canard aircraft with the MS1 airfoil, there is approximately a 3% increase in drag per degree increase in decalage angle. Unfortunately, the decrease in trim drag is small for decreases in wing aspect ratio. For the NLS airfoil, however, the decrease in drag due to decalage angle is almost zero because the drag curves are rather flat in the region of trim decalage angle. However, the same increase in drag exists with the reduction of wing aspect ratio. From this analysis, the aspect ratio for both the wing and canard was chosen to be 12, the maximum allowable.

To best optimize the total wing area and area ratios to determine the minimum trim drag, the trim decalage angle for each area ratio was plotted on separate figures which had different total areas. Figure 12 is a sample of such a figure. It shows the trim drag for the six-place canard configuration with the MS(1)-0313 airfoil at a total wing area of 12.9 m^2 (140 ft^2). This figure illustrates the increase in drag due to decalage angle, and also shows the decrease in drag obtained by increasing the stagger which decreases the trim decalage angle. For the canard design location 1.8 m (6 ft) aft of the nose, the minimum trim drag is almost equal for all area ratios. Figure 13 is another example of trim drag for the area ratios at a total wing area of 18.4 m (200 ft^2) for the six-place canard aircraft with the NL(S)-0715F airfoil. Again, the minimum trim drag is almost equal for all area ratios, and the larger stagger has the least drag because the decalage angle is less for trim. This figure, in comparison to Fig. 12, shows that in the region of trim, the drag for the NLS airfoil does not increase as rapidly as does the drag for the MS1 airfoil for increasing decalage angle.

Figure 14 shows the locus of minimum trim drag for the six-place canard aircraft. The six-place drag varies only slightly with total area and area ratios for both airfoil configured aircraft. Total lift coefficient is in the range of $0.25 < C_L < 0.7$, which is a total wing loading range of $968 < W/S < 2903$ N/m^2 $(20 < W/S < 60$ psf). Figure 14 also shows the trim drag reduction due to the forward placement of the canard and, hence, larger stagger. A 3% decrease in trim drag is gained for the aircraft.

The final configurations chosen for the canard aircraft have wing areas that yield minimum trim drag at an area ratio equal to 70/30 for the MS1 airfoil and 80/20 for the NLS airfoil. Since the trim drag for all area ratios is almost equal, it was desirable to select the highest possible area ratio, without being penalized severely for drag, so that minimum lift would be lost in a canard stall situation. Since the canard is at a greater incidence angle than the wing and the same airfoil shapes are used, the canard would always stall first, and with minimum area chosen for the canard, less total lift would be lost. Also for the 80/20 area ratio, all the fuel could be placed in the wing without any fuselage fuel cell. The drag for the 50/50 area ratio was less, but the location of the wing

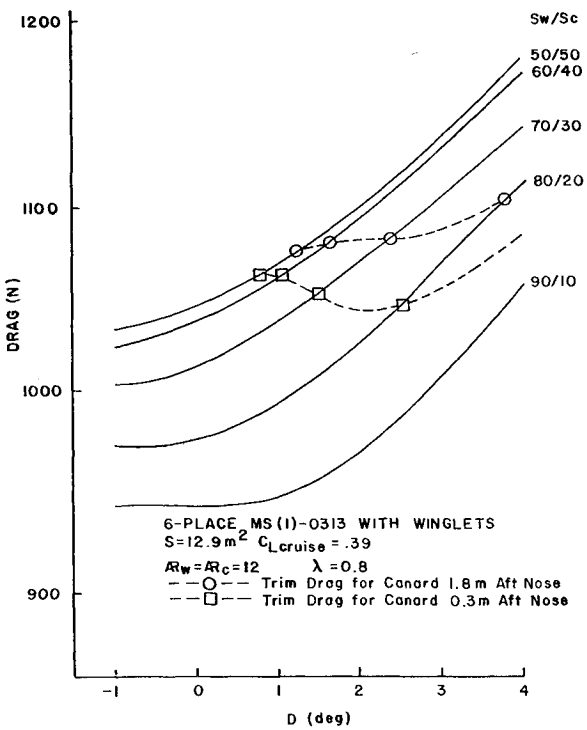

Fig. 12 Sample trim drag optimization curves for the six-place MS(1)-0313 canard aircraft.

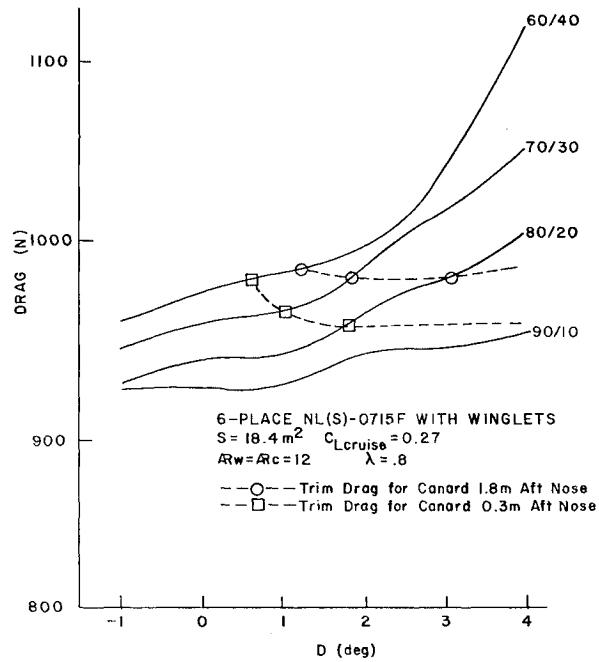

Fig. 13 Sample trim drag optimization curves for the six-place NL(S)-0715F canard aircraft.

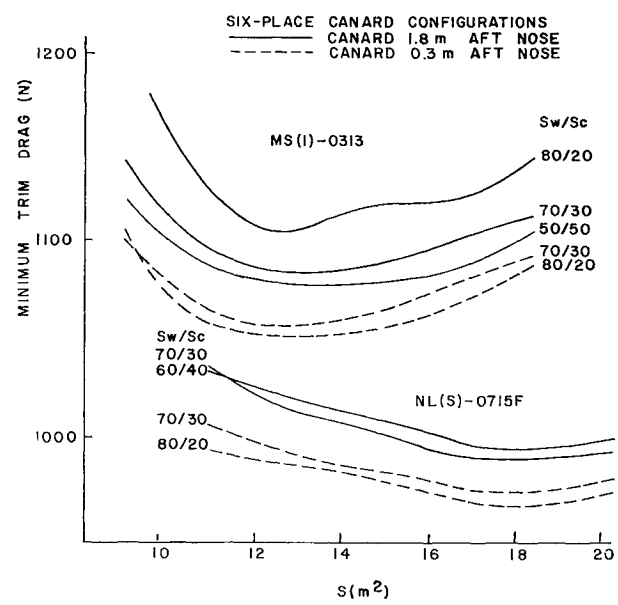

Fig. 14 Minimum trim drag for the six-place canard aircraft.

would be too far aft and could not be located feasibly on the fuselage tailcone.

Even though this study considered only the cruise flight mode for design selection, takeoff rotation was briefly reviewed. It was noted that for all configurations which could be trimmed, takeoff rotation speed was acceptable.

Figure 15 shows the exterior views of the six-place baseline and canard designs, respectively. The six-place canard design shown is configured with the NLS airfoil at an area ratio of 80/20.

Design Comparison and Concluding Remarks

Tables 2 and 3 list the final performance of the baseline and canard aircraft for the six designs. Also included in Table 2 is the performance of a typical current-technology, six-place aircraft[7] for comparison purposes. The engine weight for both the baseline and the canard was 2224 N (500 lbm).

The lift-to-drag ratios achieved by the baseline aircraft are considerably higher than those of most contemporary light and business aircraft. Holmes and Croom[7] indicate that current-technology, six-place aircraft have maximum lift-to-drag ratios of about 14 at 300 knots cruise speed. The six-place baseline aircraft of this study attained cruise lift-to-drag ratios of 19 or more at 350 mph, a 30% improvement. The improved performance can be attributed to the superior airfoil sections used on the baseline aircraft as well as to the higher aspect ratio wing with winglets found on these aircraft. Equally important, it should be remembered that these aircraft designs have cruise-matched wing loadings. The baseline aircraft all have a wing loading greater than 1451 N/m^2 (30 psf), which is a value 30% higher than that of current-technology light and business aircraft. However, the wings of the current-technology aircraft have most likely been sized based on field length requirements. The higher wing loading of these designs enables the induced drag and two-dimensional drag to approach the values of each other, thereby attaining minimum drag for the aircraft at cruise flight conditions. It should also be noted that the baseline aircraft were able to be trimmed with a small load on the horizontal tail, rather than a high download as found on some aircraft.

The cruise performance of the canard aircraft is considerably above that of current-technology aircraft, but for two of the four configurations the performance is slightly below that of the baseline designs. The poorer performance of the canard aircraft can be attributed to the high canard loading necessary in order to trim. The canard loading is approximately 2177 N/m^2 (45 psf) for the canard configurations. Since the induced drag increases with the square of the lift coefficient, the high canard loading penalizes the overall performance of the canard configurations. The minimum trim drag for the MS1 six-place configuration is 5% greater for the canard aircraft than it is for the baseline aircraft. For the NLS, the minimum trim drag is within 1% of the baseline. For off-optimum cruise conditions the canard is superior, as Fig. 8 illustrates. In addition, because of the positive decalage between the canard and wing, the canard will stall first, preventing the main wing from ever stalling and thus providing a stall-proof configuration. In Table 2 the takeoff gross weights were different between the baseline and canard configurations. Table 3 illustrates the cruise performance of the canard and baseline aircraft for equal gross takeoff weight. For this table, the fuel in the baselines has been reduced to achieve the same takeoff gross weights as

Table 2 Trimmed six-place aircraft performance

	MS(1)-0313		NL(S)-0715F		Current
	Baseline	Canard	Baseline	Canard	technology[7]
Wt, N (lb)	19,148 (4,306)	18,587 (4,179)	19,032 (4,278)	18,792 (4,225)	22,399 (5,036)
S[a], m^2 (ft^2)	13.1 (142)	12.9 (140)	12.1 (131.4)	18.4 (200)	18.9 (206)
S_W/S_C		70/30		80/20	
S_W, m^2 (ft^2)	13.1 (142)	9.0 (98)	12.1 (131.4)	14.7 (160)	18.9 (206)
S_C[b], m^2 (ft^2)	2.8 (30)	3.9 (42)	2.8 (30)	3.7 (40)	
C_L	0.429	0.387	0.458	0.274	0.33
W/S,[c] N/m^2 (psf)	1,534 (31.7)	1,297 (29.9)	1,640 (33.9)	1,021 (21.1)	1,180 (24.4)
$(W/S)_W$, N/m^2 (psf)		1,069 (22.1)		764 (15.8)	
$(W/S)_C$, N/m^2 (psf)		2,322 (48.0)		2,085 (43.1)	
Drag, N (lb)	1,032 (232)	1,085 (244)	987 (222)	983 (221)	1,601 (360)
L/D	19.44	17.1	20.04	19.2	14
$(L/D)_{max}$	21.6	18.3	23.8	23.5	
Range km (mi)	2789 (1774)	2559 (1609)	2928 (1841)	2842 (1787)	1988 (1250)
ΔRange		−9.3%		−2.9%	

[a] The baseline aircraft reference area is only the wing area and the reference area for the canard aircraft is the sum of the wing and canard areas. [b] For the baseline aircraft, S_C refers to the aft horizontal tail area, S_H. [c] Includes additional wing lift to compensate for tail load.

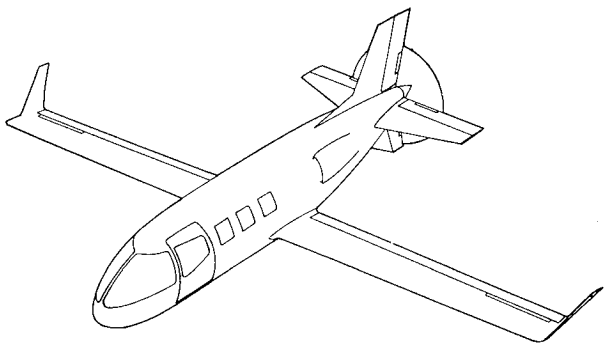

Fig. 15a Six-place baseline aircraft, exterior view.

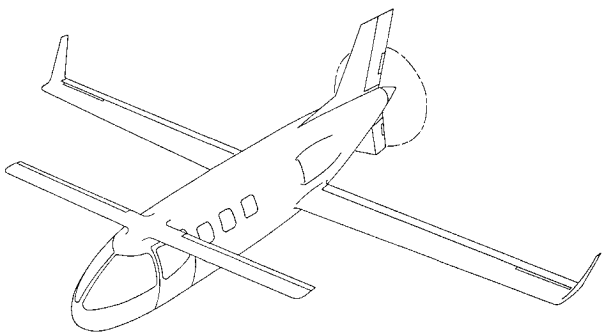

Fig. 15b Six-place canard aircraft, exterior view.

both canard configurations. The optimization and trim procedures were then repeated at these reduced weights. At a fixed gross weight, even though the baselines have lower drag than their corresponding canard configurations, the range of both canard configurations is 4-5% greater than the respective baselines. This is due to the reduced fuel carried on the conventional configurations. A similar study was conducted for a 12-passenger turbofan by Keith.[31] Similar results were obtained in the comparisons of the canard with the baseline.

Figure 8 illustrates why the cruise performance of the baseline is slightly superior to that of the canard design. It shows that zero or slightly positive trim loading for the baseline configuration is greater than the optimum trim loading for any canard configuration. The optimum trim loading is higher for the baseline with the conventional aft horizontal tail because the induced drag is less. Keith[31] has shown that the induced drag for a canard configuration with an area ratio of 80/20 is 30% higher than a single wing with an aft tail, and the induced drag is as much as 45% higher for a tandem wing system.

Ideally it would be desirable to design a fuselage for a canard aircraft such that it would allow the largest possible stagger. This is because canard configurations with larger stagger not only have less drag at a given decalage angle, but also have lower trim decalage angles, which reduce the drag even further as illustrated in Figs. 12 and 13. It would also be better to design the canard aircraft with either a smaller c.g. travel, which would allow a smaller range in C_{M_α}, or at least have the cruise configuration designed such that the c.g. would be in the most aft location so that C_{M_α} could be a maximum, and yet still less than zero. The aft c.g. would

Table 3 Trimmed six-place aircraft performance for equal gross weights

	MS(1)-0313		NL(S)-0715F	
	Baseline	Canard	Baseline	Canard
Wt, N (lb)	18,582 (4,178)	18,587 (4,179)	18,814 (4,230)	18,792 (4,225)
S^a, m^2 (ft^2)	12.7 (138)	12.9 (140)	11.9 (129.9)	18.4 (200)
S_W/S_C		70/30		80/20
S_W, m^2 (ft^2)	12.7 (138)	9.0 (98)	11.9 (129.9)	14.7 (160)
S_C^b, m^2 (ft^2)	2.8 (30)	3.9 (42)	2.8 (30)	3.7 (40)
C_L	0.428	0.387	0.458	0.274
W/S,[c] N/m^2 (psf)	1,371 (31.6)	1,297 (29.9)	1,639 (33.9)	1,021 (21.1)
$(W/S)_W$, N/m^2 (psf)		1,069 (22.1)		764 (15.8)
$(W/S)_C$, N/m^2 (psf)		2,322 (48.0)		2,085 (43.1)
Drag, N (lb)	1,014 (228)	1,085 (244)	983 (221)	983 (221)
L/D	19.16	17.1	19.93	19.2
$(L/D)_{max}$	21.6	18.3	23.8	23.5
Range, km (mi)	2,446 (1,538)	2,559 (1,609)	2,727 (1,715)	2,842 (1,787)
ΔRange, %		+4.6		+4.2

[a] The baseline aircraft reference area is only the wing area and the reference area for the canard aircraft is the sum of the wing and canard areas. [b] For the baseline aircraft, S_C refers to the aft horizontal tail area, S_H. [c] Includes additional wing lift to compensate for tail load.

allow a greater canard-to-wing moment arm ratio, which would decrease both the canard loading and the high induced drag associated with it.

It was shown that an increase in canard aspect ratio relative to the wing aspect ratio would increase $C_{L_{\alpha C}}/C_{L_{\alpha W}}$, which would decrease trim decalage angle and trim drag. From this standpoint, it would be advantageous to increase the canard aspect ratio above 12 and gain the benefit of a lower decalage angle, i.e., the lower drag associated with it. Since the canard is highly loaded, a reduction in induced drag would also occur. Consideration might also be given to two different airfoil sections on the wing and canard such that a high $C_{L_{\alpha C}}/C_{L_{\alpha W}}$ could be attained which would also decrease trim decalage angle, thereby decreasing trim drag.

This design study has shown that both the baseline and canard aircraft offer a significant improvement in cruise performance as compared to current-technology aircraft, and that for aircraft with the same gross takeoff weight the canard performance is slightly better. When these cruise performance comparisons are factored in with the advantage of a stall-proof aircraft and improved off-design performance, the canard aircraft offers a very attractive cruise performance package for general aviation applications.

Future work is needed with different airfoils on the canard and wing as well as structural optimization of the fuselage weights for canard-wing loading.

Acknowledgments

The results presented in this paper were obtained from research funded by NASA Research Grant NAG1-26, administered by Langley Research Center under the direction of Dr. Bruce Holmes.

References

[1] Rutan, B., "Development of Small High-Aspect-Ratio Canard Aircraft," *The Society of Experimental Test Pilots,* Vol. 15, No. 2, 1980.

[2] Rutan, B., "Tale of the Three EZ's," *Sport Aviation,* Vol. 29, No. 2, Feb. 1980.

[3] Laitone, E.V., "Ideal Tail Load for Minimum Aircraft Drag," *Journal of Aircraft,* Vol. 15, March 1978, pp. 190-192.

[4] Goldstein, S.E. and Combs, C.P., "Trimmed Drag and Maximum Flight Efficiency of Aft Tail and Canard Configurations," AIAA Paper 74-69, 1974.

[5] Wolkovitch, J., "Subsonic VSTOL Aircraft Configurations with Tandem Wings," *Journal of Aircraft,* Vol. 16, Jan. 1974, pp. 605-611.

[6] Tulinius, J.R. and Margason, R.J., "Aircraft Aerodynamic Design and Evaluation Methods," AIAA Paper 76-15, 1976.

[7] Holmes, B.J. and Croom, C.C., "Aerodynamic Design Data for a Cruise-Matched High Performance Single Engine Airplane," SAE Paper 810625, 1981.

[8] Benstein, E.H. and Smith, R., "Advanced General Aviation Turbine Engine (GATE) Study," NASA CR-159624, June 1979.

[9] Nicolai, L.M., *Fundamentals of Aircraft Design,* METS, Inc., San Jose, Calif., 1975, pp. 5.1-5.24, pp. 20.1-20.24.

[10] Torenbeek, E., *Synthesis of Subsonic Airplane Design,* Delft University Press, Delft, Holland, 1976, pp. 27-76, pp. 263-302, p. 352.

[11] Torenbeek, E., "Prediction of Wing Group Weight for Preliminary Design," *Aircraft Engineering,* July 1971.

[12] Hayes, B., Lopez, R., and Rhodes, M., "General Aviation Light Turbo-Powered Aircraft," UMR Senior Design Project, 1980.

[13] "Evaluation of Torenbeek's Weight Estimating Formula for a Range of Aircraft Wings," NASA-Internal Memo.

[14] Somnay, Rajesh J., "Design of Dual Wing Structures," UMR Thesis, Rolla, Mo., Aug. 1983.

[15] Thwaites, B., "Approximate Calculation of the Laminar Boundary Layer," *Aeronautical Quarterly,* Vol. 1, 1949, pp. 245-280.

[16] Michel, R., "Etude de la Transition sur les Profiles d'Aile; Establissement d'un Critere de Determination de Point de Transition et Calcul de la Trainee de Profile Incompressible," ONERA Rept. 1/1578A, 1951.

[17] Cebeci, T. and Bradshaw, P., *Momentum Transfer in Boundary Layers,* Hemisphere Publishing Corp., Washington, 1977, pp. 192-194.

[18] Cebeci, T. and Smith, A.M.O., "Calculation of Profile Drag of Airfoils at Low Mach Numbers," *Journal of Aircraft,* Vol. 5, Nov.-Dec. 1968, pp. 535-542.

[19] McGhee, R.J., "Wind Tunnel Results for a 13-Percent-Thick Medium Speed Airfoil Section," (NASA TM in publication).

[20] Somers, D.M., Data on general aviation natural laminar flow airfoil, to be published by NASA.

[21] Tulinius, J., "Unified Subsonic, Transonic, and Supersonic NAR Vortex Lattice," TFD-72-523, North American Rockwell, Los Angeles, Calif., 1972.

[22] Paulson, J.W., "Application of Vortex Lattice Theory to Preliminary Aerodynamic Design," NASA Langley Research Center, Langley Station, Va., 1976.

[23] Roskam, J., *Methods for Estimating Drag Polars of Subsonic Airplanes,* published by the author, Lawrence, Kansas, 1971, p. 2.3.

[24] Hoerner, S.F., *Fluid Dynamic Drag,* published by the author, 1965, pp. 6.15-6.19.

[25] Crawford, D.R., *A Practical Guide to Airplane Performance and Design,* 1st ed., Crawford Aviation, Torrance, Calif., 1979, p. 174.

[26] Holmes, B.J., "Aerodynamic Design Optimization of a Fuel Efficient High Performance, Single-Engine, Business Airplane," AIAA Paper 80-1846, April 1981.

[27] Loftin, L.D. Jr., "Subsonic Aircraft, Evolution and the Matching of Size to Performance," NASA RP 1060, 1980.

[28] Whitcomb, R.T., "A Design Approach and Selected Wind-Tunnel Results at High Subsonic Speeds for Wing-Tip Mounted Winglets," NASA TN D-8260, 1976.

[29] Roskam, J., *Methods for Estimating Stability and Control Derivatives of Conventional Subsonic Airplanes,* published by the author, Lawrence, Kansas, 1971, pp. 21-12.2.

[30] Roskam, J., *Airplane Flight Dynamics and Automatic Flight Controls, Part I,* Roskam Aviation and Engineering Corp., 1979, pp. 243-377.

[31] Keith, M.W., "Parametric Canard/Wing Aerodynamic Trade-Off Analysis and Trim Design Comparison of Canard and Conventional High Performance General Aviation Configurations," UMR Thesis, Rolla, Mo., 1982.

[32] Kuhlman, J.M., "Iterative Optimal Subcritical Aerodynamic Design Code Including Profile Drag," AIAA Paper 83-0012, 1983.

[33] Mason, W.H., "Wing-Canard Aerodynamics at Transonic Speeds—Fundamental Considerations on Minimum Drag Spanloads," AIAA Paper 82-0097, 1982.

[34] Kroo, I.M. and McGeer, T., "Optimization of Canard Configurations—An Integrated Approach and Practical Drag Estimation Method," ICAS 13th Congress and AIAA Aircraft Systems and Technology Conference, ICAS 82-6.8.1, 1982.